minerals

MDPI

Article

Advancing the Understanding of Sediment Contamination Dynamics in the Iron Quadrangle (Brazil): A Comparative Analysis of Pollution Indices for PTE Assessment

Raphael Vicq [1,*], Mariangela G. P. Leite [2], Lucas P. Leão [2], Hermínio A. Nallini Júnior [2], Patricia Gomes [1], Rita Fonseca [3] and Teresa Valente [1,*]

1 Earth Sciences Department, Institute of Earth Sciences, University of Minho, 4710-057 Braga, Portugal; patriciagomes@dct.uminho.pt
2 Department of Geology, Federal University of Ouro Preto, Morro do Cruzeiro Campus, Ouro Preto 35400-000, MG, Brazil; mgpleite@gmail.com (M.G.P.L.); lucas.leao@ufop.edu.br (L.P.L.); nalini@ufop.edu.br (H.A.N.J.)
3 Earth Science Institute, University of Évora, Largo Dos Colegiais 2, 7004-516 Évora, Portugal; rfonseca@uevora.pt
* Correspondence: raphaelcosta@dct.uminho.pt (R.V.); teresav@dct.uminho.pt (T.V.)

Abstract: The assessment of sediment contamination is a critical component in understanding the dynamics of potentially toxic elements (PTEs) in aquatic ecosystems, particularly in regions with intensive mining activities. This study focuses on the Rio das Velhas basin, located in the Iron Quadrangle (IQ), one of the most important mining provinces in the world, characterized by extensive anthropogenic pressures and rich geological diversity. A comprehensive evaluation of sediment contamination in this region was conducted, applying multiple univariate and multielement indices, including the contamination factor (CF), enrichment factor (EF), modified contamination degree (mCd), pollution index (PI), modified pollution index (MPI), and ecological risk index (RI). A high sampling density (1 sample per 15 km^2) enabled the creation of geochemical maps and the identification of contamination hotspots. The results revealed that As and Cd are the most concerning elements, with concentrations exceeding regional background levels. While EF provided a more sensitive and comprehensive spatial distribution of contamination, MPI emerged as a robust index for capturing geochemical trends in complex environments. The study also highlighted that over 20% of the samples exceeded guideline values for sediment quality, posing ecological risks. Elevated concentrations of PTEs, particularly As and Cd, raise concerns about their potential mobilization and bioaccumulation, threatening aquatic ecosystems. These findings underscore the urgent need for enhanced monitoring and targeted management strategies in mining-impacted basins. This work not only advances the understanding of sediment contamination dynamics in the IQ but also establishes a methodological framework for evaluating sediment quality in heavily impacted mining regions worldwide.

Keywords: environmental risk assessment; pollution indices; mining impact; geochemical mapping; Velhas River basin

check for updates

Academic Editors: María de la Luz García Lorenzo, José María Esbrí and Oscar Andreu Sánchez

Received: 19 January 2025
Revised: 8 February 2025
Accepted: 11 February 2025
Published: 20 February 2025

Citation: Vicq, R.; Leite, M.G.P.; Leão, L.P.; Nallini Júnior, H.A.; Gomes, P.; Fonseca, R.; Valente, T. Advancing the Understanding of Sediment Contamination Dynamics in the Iron Quadrangle (Brazil): A Comparative Analysis of Pollution Indices for PTE Assessment. *Minerals* **2025**, *15*, 199. https://doi.org/10.3390/min15030199

Copyright: © 2025 by the authors. Licensee MDPI, Basel, Switzerland. This article is an open access article distributed under the terms and conditions of the Creative Commons Attribution (CC BY) license (https://creativecommons.org/licenses/by/4.0/).

1. Introduction

Sediments are among the most sensitive environmental compartments to contamination by potentially toxic elements (PTEs), mainly due to their high adsorption/desorption capacity. This property is primarily attributed to clay minerals and iron and aluminum

oxides–hydroxides in the clay size fraction, which facilitate the accumulation and binding of PTEs [1]. As a result, sediments act as critical geochemical reservoirs for toxic elements and play a key role in their distribution and bioavailability in aquatic ecosystems [2].

Studies show that more than 90% of the total PTE concentration in river environments is typically sequestered in sediments [3,4]. Consequently, sediments serve as a controlling matrix for the mobility, availability, and eventual transfer of these substances to the hydrosphere and/or biota. This dynamic poses potential risks to ecosystems and human health, as many metals and metalloids are known to be toxic and carcinogenic [4–6].

Beyond contamination, sediments serve as natural archives of recent environmental change [7], providing a historical record of pollution and allowing spatial analyses to determine the patterns of contamination distribution patterns in aquatic systems [8–10]. This role is crucial in heavily industrialized or anthropogenically affected regions. For example, studies in mining-affected basins show significantly elevated PTE concentrations in river sediments compared to regional backgrounds or crustal averages [9–12]. This trend is demonstrated by the Velhas River basin, located in Brazil's Iron Quadrangle (IQ), one of the most important mineral provinces in the world.

Sediment Quality Control Guidelines (SQCQs) are widely employed to assess sediment pollution. These guidelines estimate the degree of contamination and the potential adverse effects of PTE on aquatic organisms [13,14]. However, sediment quality indicators can often achieve a more comprehensive understanding of geochemical trends [10,15]. These tools classify sediment quality based on specific PTE concentrations and offer valuable insight into contamination levels. Several methods have been developed to quantify metal enrichment and accumulation in sediments, allowing the classification of contamination levels and their associated impacts [16–19]. Typically, these methods involve comparing observed concentrations with regional background values, as well as average crustal concentrations. Ecological indices further complement this analysis by integrating contamination levels with ecological risks, providing a holistic evaluation of the status of aquatic systems [17,20].

The upper course of the Velhas River basin, within the IQ, has been the subject of numerous geochemical studies due to its extensive mining legacy, present activity, and diverse geological framework [11,21–26]. Despite substantial research efforts, existing studies often lack sufficient sampling density and fail to incorporate comprehensive multielement sediment quality assessments. As a result, the broader environmental and ecological impacts of sediment contamination in this region remain inadequately explored.

To address these limitations, this study undertakes a detailed evaluation of the environmental quality and ecological health of the sediments in the upper course of the Velhas River. A set of ecological indicators—including the contamination factor (CF), enrichment factor (EF), modified contamination degree (mCd), pollution index (PI), and modified pollution index (MPI)—is applied to characterize the contamination levels and risks.

Additionally, high-density geochemical maps are generated, providing spatially explicit information on sediment contamination patterns and intensity. This comprehensive approach aims to enhance the understanding of contamination dynamics in the Iron Quadrangle while establishing a robust framework for monitoring and managing sediment quality in heavily impacted mining regions.

2. Materials and Methods

2.1. Study Area

The upper Velhas River region is located in the Iron Quadrangle, a major mining region in Minas Gerais, Brazil, covering an area of 3200 km^2. This area includes nine towns: Rio Acima, Itabirito, Nova Lima, Ouro Preto, Raposos, Caeté, Belo Horizonte, Sabará, and Santa Luzia. It supplies water to the metropolitan area of Belo Horizonte, which has more

than 5.7 million inhabitants, making it the third-largest urban center in Brazil [27]. The river basin is bordered by Belo Horizonte to the north, Ouro Preto to the south–southeast, Serra da Moeda to the west, and Serra da Piedade to the east (Figure 1). The Velhas River and its tributaries cross areas of varying land use, from forested areas to highly urbanized and mined regions.

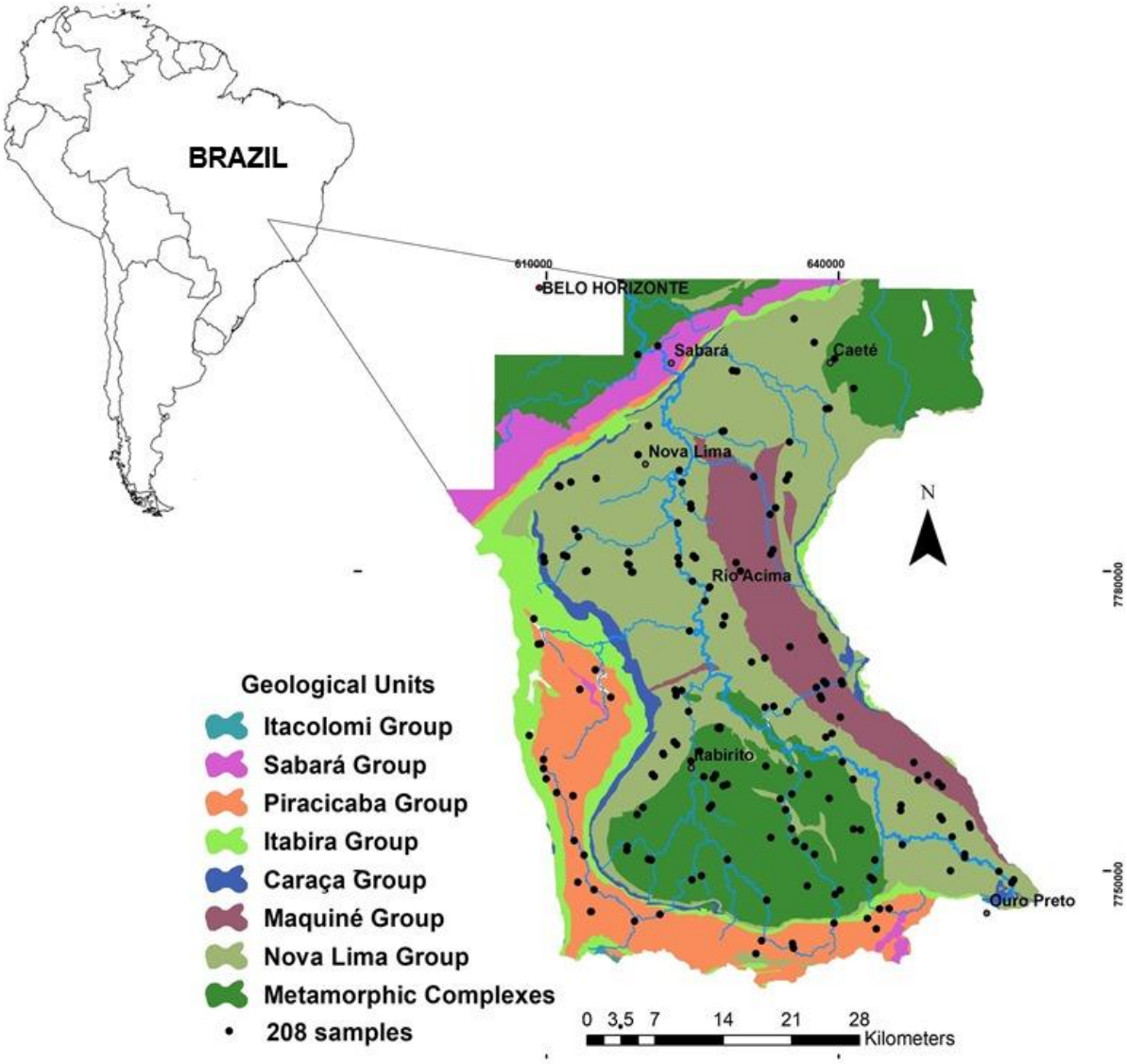

Figure 1. Simplified geological map of the upper Velhas River basin.

The presence of such economically significant deposits is the result of the region's geological diversity, which includes Archean and Proterozoic rocks (Figure 1). The IQ is recognized for its geological diversity and complexity, encompassing a variety of lithostratigraphic units that offer insights into the region's tectonic, sedimentary, and metamorphic history.

The geology of the basin is thought to be organized into four major lithostratigraphic units, from oldest to youngest: (i) Metamorphic complexes, which constitute the crystalline basement, composed of poly-deformed gneissic rocks of tonalitic composition and granite, granodiorite, mafic, and ultramafic intrusions forming the Bonfim, Santa Rita, Caeté, Belo Horizonte, Santa Bárbara, and Bação complexes [28,29]; (ii) the Rio das Velhas supergroup, composed of metasedimentary and metavolcanic rocks [30,31], subdivided into two groups: Nova Lima and Maquiné. The Nova Lima group predominantly features

volcano–sedimentary rocks such as carbonate schists, metacherts, banded iron formations, and phyllites. The Maquiné group includes a basal unit of metaconglomerates, overlain by massive and sericitic quartzites, sericite–quartz–schists, and phyllites [31]; (iii) the Minas supergroup is up to 6000 m thick, composed mainly of pelitic and quartzose metasediments, placed discordant above the Rio das Velhas green belt, and subdivided into four groups that record a progression of depositional environments, including the Caraça group (basal metaconglomerates and metarenites, indicating fluvial to shallow marine conditions), Itabira group (composed of chemical sediments, particularly BIFs, marking a period of significant iron deposition), the Piracicaba group (metapelites and additional chemical sedimentary sequences), and the Sabará group (the youngest unit, consisting mainly of terrigenous sediments, with a basal conglomeratic phyllite, indicating a more dynamic sedimentary regime during the late stages of basin evolution) [31]; (iv) the Itacolomi group, which comprises quartzites and metaconglomerates that represent fluvial-deltaic to shallow marine environments; (v) and Tertiary and Quaternary deposits, representing the ongoing sedimentary processes within the region, thus typically associated with modern fluvial systems and weathering profiles [30].

The economy of the region is mainly based on mining activities (iron, gold, limestone, dolomite, bauxite, manganese, and topaz), as well as the steel industry and tourism [32].

Mining activities, particularly for iron and gold ores, have had a significant impact on the basin, contributing to widespread sediment contamination and environmental problems. The combination of mining, urbanization, and industrial activities highlights the need for comprehensive environmental monitoring in this region.

Gold is the primary mineral resource extracted in the Alto Rio das Velhas region, predominantly associated with the volcanic–sedimentary sequences of the Nova Lima group, which hosts Brazil's most significant gold district. The Cuiabá, Morro Velho, and Raposos mines contain the largest gold reserves in the region, with estimated resources of 11.20, 6.60, and 4.30 million tonnes, respectively, and average gold grades of 8.49, 10.00, and 6.27 g per tonne [33]. As by-products of gold extraction, all active mines produce silver, sulfur, and arsenic. Arsenic concentrations range between 3.07 and 8.87 mg/kg, while sulfur concentrations vary between 6.61% and 9.06%. Additionally, gold mineralization is associated with the conglomerate lenses of the Maquiné group. Beyond gold, the region also hosts significant deposits of serpentinites from the Córrego dos Boiadeiros complex and ultramafic rocks from the Quebra-Osso group, both widely used as smelting materials [34].

Regarding iron ore, the region contains high-grade iron ore bodies, typically with iron (Fe) content above 64%. Enriched itabirites, with Fe concentrations ranging from 30% to 60%, are also mined. Major active deposits include the Água Limpa (Itabirito), Vargem Grande (Nova Lima), Fábrica and Fábrica Nova (Ouro Preto and Congonhas), and Casa de Pedra (Congonhas) mines [35]. Over the past 30 years, these deposits have been extensively exploited, with an estimated annual production of 190 million tonnes (Mt). In terms of mining waste, it was reported that, in 2016, approximately 295 Mt of tailings were stored in dams, while 183 Mt of waste was deposited in open-air storage sites [36].

2.2. Sampling Procedures

To achieve a high sampling density, sediments were collected at the mouth of all 3rd-order basins within the region [37], as defined using ArcGIS 10.8 software. The selection process involved overlaying the hypsometric, topographic, and hydrographic maps at a 1: 25,000 scale, provided by the Institute of Water Management (IGAM) and the Company of Mineral Resources Production (CPRM). This approach results in the collection of 208 stream sediment samples, achieving a density of approximately one sample per 15 km^2.

To account for the channel geomorphological variability, nine subsamples were collected along a stretch of 250 to 500 m of each sampling site, representing distinct geomorphological patterns, such as riffles, pools, and transitional areas. Samples were taken from the right margin, left margin, and center of the channel. Margin samples were collected at a depth of 0.50 m from the riverbed. The subsamples were mixed in the field to create a composite sample representative of the site. The homogenized material was quartered to obtain a 500 g composite sample, which was stored in labeled plastic bags and transported to the laboratory under refrigerated conditions to preserve its integrity [38,39].

2.3. Chemical Analyses and Quality Control

The sediment samples were air-dried and sieved, and 1 g of the fraction smaller than 63 µm was subjected to aqua regia digestion (HCl with HNO_3, in a 3:1 ratio) at the Laboratory of Geochemistry of the Federal University of Ouro Preto. The process was begun by adding a small volume of Milli-Q water to form a sediment "pulp". Subsequently, 7.0 mL of concentrated HCl and 2.3 mL of concentrated HNO_3 (Merck p.a.) were added to each sample. The samples were left to react in a fume hood for 16 h, followed by heating on a hot plate at 100 ± 5 °C for two hours to reduce the volume. After cooling, the samples were filtered through 0.45 µm pore filter paper, and the final volume was adjusted to 100 mL with Milli-Q water in a volumetric flask [39].

The digested samples were analyzed using a spectrophotometer of atomic emission with an inductively coupled plasma source (ICP-OES), a brand called Spectro/Model Ciros CCD. The instrument was used to quantify the concentrations of elements, such as Al, As, Ca, Cd, Co, Cr, Cu, Fe, K, Mg, Mn, Na, Ni, Pb, Ti, and Zn.

The digestion with aqua regia is known as pseudo-total digestion, extracting elements from the non-silicate fraction. This method captures trace elements of significant environmental interest, including those associated with oxides, sulfides, clay minerals, and organic matter [40–42]. To ensure robust and reliable data, quality assurance measures included the preparation of a blank for every ten samples and the duplicate analysis of 10% of the samples. Accuracy was verified by comparing results against certified reference material LKSD-01 (CCNRP-Ottawa, Canada). Recovery rates ranged between 93.3% and 102.5% (Table 1), indicating satisfactory precision and reliability.

Table 1. Percentage recovery rates for elements in certified reference material (LKSD-01—CCNRP-Ottawa, Canada).

Element	Measured Concentrations ($mg \cdot kg^{-1}$)	Certified Value LKSD 01 ($mg \cdot kg^{-1}$)	Recovery Rates (%)
As	29.2 ± 0.8	30	97.3
Cd	1.14 ± 0.02	1.2	95
Cr	11.2 ± 0.3	12	93.3
Cu	45.1 ± 1.2	44	102.5
Pb	83.4 ± 2.6	84	99.3
Zn	330.3 ± 9.3	337	98

2.4. Pollution Quantification Indices

2.4.1. Contamination Factor (CF)

The CF calculation was performed using Equation (1) [17]:

$$CF = \frac{C_{PTE}}{C_{background}} \quad (1)$$

where C_{PTE} represents the concentration of PTE in the sediments of the Velhas River basin, and $C_{background}$ corresponds to the background value of the same element in the basin. The background values adopted as reference were As = 20.6 mg·kg^{-1}; Cd = 1.02 mg·kg^{-1}; Pb = 28.4 mg·kg^{-1}; Cu = 37.9 mg·kg^{-1}; Cr = 151.3 mg·kg^{-1}; Ni = 56.9 mg·kg^{-1}; and Zn = 63.1 mg·kg^{-1} [43]. The adoption of regional reference values is especially recommended in complex geological environments [44].

This index is among the simplest methods for evaluating sediment contamination. It categorizes contamination into four qualitative levels based on the CF value:

- CF < 1: low contamination;
- 1 < CF < 3: moderate contamination;
- 3 < CF < 6: considerable contamination;
- CF > 6: very high contamination.

2.4.2. Enrichment Factor (EF)

This index normalizes PTE concentrations by comparing the region's reference concentrations with a reference metal, called a normalizing element, allowing for more effective comparison, especially in regions with older soils and sediments and with great geological diversity [44]. Although iron (Fe) is commonly used as a normalizing element, its high background value in the Rio Velhas basin (166,000 mg·kg^{-1}) [40]—four times higher than the average value in the upper crust [45]—may lead to the underestimation of FE values [46]. In this study, aluminum (Al) was selected as the normalizing element [46,47] due to its low natural mobility and role as a primary constituent of clay minerals found in river sediments [48–50]. EF for each element was calculated according to Equation (2) [51]:

$$EF = \frac{\frac{Ci}{C_{Al}}}{\frac{Bi}{B_{Al}}} \quad (2)$$

where,

- Ci is the concentration of each element in the sediment sample;
- C_{Al} is the concentration of the normalization element, in this case aluminum (Al), in the same sediment sample;
- Bi is the reference geochemical background value of each element;
- B_{Al} is the reference geochemical background value of the reference element, aluminum (Al).

Five qualitative categories are used to describe the enrichment levels, as summarized in Table 2.

Table 2. Enrichment factor (EF) classes.

Class	Value	Description—Sediment Enrichment
1	EF < 2	No enrichment/natural influence
2	2 < EF < 5	Moderate enrichment
3	5 < EF < 20	Severe enrichment
4	20 < EF < 40	Very severe enrichment
5	EF > 40	Extremely severe enrichment

The enrichment factor (EF) can provide insight into how to differentiate an anthropogenic source from a natural process. EF values close to 1 indicate a crustal source, while values greater than 10 are related to anthropogenic sources and/or processes [51].

2.4.3. Modified Contamination Degree (mCd) and Modified Pollution Index (MPI)

Multielement indices were developed to address the limitations of pollution indices based on single elements. The modified contamination degree (mCd) and pollution index (PI) provide more comprehensive assessments by integrating data from multiple PTEs [17,52]. Building on these, the modified pollution index (MPI) was introduced [53], incorporating the enrichment factor (EF) into its calculation for a more nuanced evaluation of contamination levels. These indices are calculated using Equations (3)–(5). Table 3 presents the quality classification ranges for the multielement indices.

$$\mathrm{mCd} = \frac{\sum_{i=1}^{n} \mathrm{cf}^{i}}{n} \tag{3}$$

$$\mathrm{PI} = \frac{\sqrt{(\mathrm{Cf\ average})^{2} + (\mathrm{Cfmax})^{2}}}{2} \tag{4}$$

$$\mathrm{MPI} = \frac{\sqrt{(\mathrm{Ef\ average})^{2} + (\mathrm{Efmax})^{2}}}{2} \tag{5}$$

Table 3. Thresholds for sediment quality classification for multielement indices.

Class	Sediment Qualification	mCd	PI	MPI
0	Unpolluted	mCd < 1.5	PI < 0.7	MPI < 1
1	Slightly polluted	1.5 < mCd < 2	0.7 < PI < 1	1 < MPI < 2
2	Moderately polluted	2 < mCd < 4	1 < PI < 2	2 < MPI < 3
3	Moderately–heavily polluted	4 < mCd < 8	----	3 < MPI < 5
4	Severely polluted	8 < mCd < 16	2 < PI < 3	5 < MPI < 10
5	Heavily polluted	16 < mCd < 32	PI > 3	MPI > 10
6	Extremely polluted	mCd > 32	---	----

2.4.4. Ecological Risk and Potential Ecological Risk

The potential ecological risk index (RI) evaluates the sensitivity of the biological community at a given site by considering the toxicity and environmental effects of individual elements [15]. This index compares the concentration of the element in the local samples with regional reference values, adjusting for a factor known as the biological toxic response. This factor reflects the relative toxicity of each element and varies as follows: As = 10; Cu = Pb = 5; Zn = 1; Cr = Ni = 2; Cd = 30 [15,17]. The formula for the potential ecological risk of an individual element is expressed in Equation (6).

$$\mathrm{RI} = \sum_{i=1}^{n} \mathrm{Er}^{i} = \sum_{i=1}^{n} \mathrm{Tr}^{i} \times \mathrm{Cf}^{i} \tag{6}$$

where,

- Er^{i} is the potential ecological risk index of an individual element;
- Tr^{i} is the biological toxic response factor of an individual element;
- Cf^{i} is the contamination factor for each single element.

The overall RI aggregates the individual risks to provide a comprehensive assessment of ecological vulnerability. This index categorizes ecological risk into four levels, ranging from low to very high, as summarized in Table 4.

Table 4. Potential and modified ecological risk index classification grades.

Er^i	Ecological Grade (Er^i)	RI	Ecological Grade (RI)
$Er^i < 40$	Low risk	RI < 150	Low risk
$40 < Er^i < 80$	Moderate risk	150 < RI < 300	Moderate risk
$80 < Er^i < 160$	Considerable risk	300 < RI < 600	Considerable risk
$160 < Er^i < 320$	High risk	----	----
$Er^i > 320$	Very high risk	RI > 600	Very high risk

2.4.5. Mapping of Pollution Indices

Maps with several indices were prepared using ArcGIS 10.8 software, adopting the World Geodetic System 1984 (WGS84) datum and the IDW (inverse distance weighted) geostatistical interpolation tool.

3. Results and Discussion

Table 5 presents the statistical parameters for element concentrations in 208 sediment samples from the upper Velhas River basin and compares these concentrations with similar studies conducted in the IQ. Table 6 provides additional context by comparing these concentrations to those observed in rivers worldwide, along with the threshold effect concentration level (TEL) and probable effect level (PEL).

Table 5. Descriptive statistics of sediment samples from the upper Velhas River and comparison of PTEs concentration with similar studies in the IQ, Minas Gerais, Brazil.

Element	Unit	Min	Max	Mean	Median	APA Sul (2005) [24] Min–Max	Pereira et al. (2007) [23] Min–Max	Gonçalves (2010) [25] Min–Max	Mendonça (2012) [26] Min–Max
As	$mg \cdot kg^{-1}$	1.6	1691	32.3	1.6	4–873	2–580	1.6–167	1.6–69
Cd		0.4	14.7	1.13	0.4	1.6–12.2	----	----	----
Cr		6.5	572	115	92.8	44–1077	30–510	197–632	8–198
Cu		0.3	234	27.7	22.3	17–841	20–110	8–97	0.3–180
Mn		41	10,053	1317	756		----	----	----
Ni		1.2	157	36.3	30.5	10–332	----	65–220	0.6–47
Pb		0.4	70.2	22.5	20.2	7–47	----	1–50	1–47
Zn		18.6	181	53.8	48.7	28–175	----	50–131	30–119

All analyzed elements showed skewed distributions, with a median consistently lower than the mean. The disparity between these two values was particularly pronounced for As, with the mean approximately 20 times higher than the median. This highlights the probable influence of localized enrichment in the dataset.

The elements with the highest variability were As, Ni, Cu, and Pb, with maximum concentrations of two to three orders of magnitude greater than their respective minimum values. In contrast, Cd and Zn displayed more uniform concentrations.

The abundance sequence of PTEs in the basin followed the order Cr > Zn > Ni > As > Cu > Pb > Cd, which differs from the typical sequence in the Earth's crust (Cr > Ni > Zn > Cu > Pb > As > Cd). As and Cd stand out, with average concentrations 16 and 11 times higher than their crustal averages, respectively [54]. Pb and Cu were also slightly elevated, with concentrations 1.5 times above their crustal abundances.

Compared to global rivers affected by mining and other anthropogenic activities (Table 6) the Velhas River basin displayed alarming PTEs concentrations. The maximum As concentration (1691 mg/kg) was the highest among all datasets considered, while the average As concentration (32.3 mg/kg) exceeded the maximum values reported for rivers such as the Liaohe, Luanhe, Luan, and Yangtze Rivers (China), the South Plate River (United States), and the Tigris River (Turkey). Similarly, the maximum concentrations of Cd and Cr in the Velhas River sediments surpassed the extreme values observed in

most other river systems. This study revealed maximum concentrations higher than those documented in previous research within the same basin, likely due to the higher sampling density. Therefore, this comprehensive sampling approach allowed for a more detailed characterization of localized contamination hotspots.

Table 6. PTEs concentrations in sediment samples from various rivers around the world and TEL (threshold effect concentration level) and PEL (probable effect level) values.

River/Location	As	Cd	Cr	Cu	Pb	Zn
Liaoche River, China [55]	9.9	1.2	35.1	17.8	10.6	50.2
Luanhe River, China [1]	3.4–13.6	0.02–0.24	11.6–76.2	9.6–35.6	23–43.7	12.9–94.7
Yangtze River, China [56]	9.1	0.2	79.1	24.7	23.8	82.9
Tigris River, Turkey [57]	2–85	0.7–3	28.4–163.4	11.2–297	62–392.4	60–247
Danubio River, Europe [58]	8.1–388	1.1–32.9	26.5–556.5	31.1–8088	14.7–542	78–2010
Axios River, Greece [59]	1–40	1–11	39–180	14–93	11–140	42–271
South Plate River, USA [60]	2.8–31	0.1–22	33–71	18–480	19–270	82–3700
Rimac River, Peru [61]	21–1543	0.5–31	24–71	51–796	62–2281	160–8076
Luan River, China [62]	2–12.9	0.03–0.37	28.7–152.7	6.5–179	8.6–38.3	21–25.7
S. Domingos, Portugal [63]	-	1.2	78.9	331.2	3307	168.8
TEL [64]	5.9	0.6	37.3	35.7	35.8	123
PEL [64]	17	3.5	90	197	91.3	315

Comparisons with the Guideline Values for Sediment Quality (GVSQs) [64] revealed important exceedances for several elements. Cr, As, Cu and Cd concentrations exceeded the TEL and PEL values in 57.9%, 33.3%, 32,7%, and 1.6% of the samples, respectively, suggesting a high potential for harmful effects on aquatic organisms interacting with the river sediments. For Pb, none of the samples exceeded the PEL value, but 16.9% of the samples exceeded the TEL. The average concentrations of As and Cr were above the PEL and that of were between the TEL and PEL thresholds, indicating a substantial ecological problem. This pattern highlights the pressing need for targeted mitigation strategies in the study basin, particularly As, Cr, and Cd.

3.1. Sediment Quality Assessment by Single Pollution Indexes

3.1.1. Contamination Factor (CF)

Table 7 summarizes the results of the CF for each PTE. Except for Cr, Pb, and Zn, all the analyzed PTEs showed at least one sampling point classified as having high contamination.

Table 7. Minimum and maximum CF values for PTEs and percentage of samples in each CF class—Velhas River basin.

	As	Cd	Cr	Cu	Pb	Zn
Minimum	0.08	0.4	0.04	0.01	0.01	0.3
Maximum	84.1	14.4	3.8	6.2	2.5	2.9
Percentage of Element Samples by Class						
Absence of Contamination	71.5	70.7	71.6	72.1	72.7	71.6
Moderate Contamination	16.9	22.9	26.8	26.2	27.3	28.4
Considerable contamination	4.9	3.9	1.6	1.1	0.0	0.0
High Contamination	6.7	2.5	0.0	0.6	0.0	0.0

The highest CF values were recorded for As and Cd, with 11.6% of the samples indicating considerable contamination for As and 6.4% for Cd. For other elements, less than 2% of samples exhibited CFs in this contamination range. However, moderate contamination was prevalent in over 25% of the samples for Cu, Cr, Pb, and Cd, underscoring the widespread impact of these elements.

3.1.2. Enrichment Factor (EF)

Table 8 shows the percentages of samples classified in each class for the enrichment factor (EF). Except for Cr and Zn, all the analyzed PTEs show at least one point with very high enrichment.

Table 8. Minimum and maximum EF values for PTEs and percentage of samples in each EF class—Velhas River basin.

	As	Cd	Cr	Cu	Pb	Zn
Minimum	0.03	0.2	0.04	0.02	0.03	0.17
Maximum	226.5	21.9	18.8	24.5	25.6	13.5
Percentage of Element Samples by Class						
No enrichment	68.3	61.2	61.2	61.8	64.5	53.5
Moderate enrichment	18.0	26.8	29.0	27.9	21.9	32.9
Severe enrichment	9.3	10.4	9.8	9.8	13.1	13.6
Very severe enrichment	2.2	1.6	0.0	0.5	0.5	0.0
Extremely severe enrichment	2.2	0.0	0.0	0.0	0.0	0.0

The enrichment factor (EF) values (Table 8) reveal varying levels of enrichment for all analyzed PTEs in the Velhas River basin, with Pb, Zn, As, and Cd showing the most severe enrichments. Notably, Pb and Zn exhibited severe enrichment in more than 13% of the samples, while As and Cd showed 9.3% and 10.4%, respectively. Cr and Cu followed closely, with 9.8% of samples classified under the severe enrichment category.

A maximum EF of 226.5 was observed for As, with 4.4% of samples classified as severe to extremely severe enrichment. Cd, Cu, and Pb also showed enrichment in this range, though at much lower frequencies (1.6% for Cd and 0.5% for Cu and Pb).

The enrichment pattern indicates localized contamination hotspots within the Velhas River basin. Regional background values for EF calculations instead of global crustal averages ensure a more accurate representation of local geochemical conditions [43,47,54]. If global averages were used, the proportion of samples classified as contaminated would significantly increase.

The EF results highlight As as a major contaminant, with its severe enrichment values requiring particular attention. Pb and Zn also demonstrate notable enrichment, suggesting potential anthropogenic contributions, such as the historical mining activities in this basin.

3.2. Spatial Distribution of Quality Indexes (EF and CF)

Figure 2a,b illustrate the spatial distributions of univariate sediment quality indices, highlighting locations with CF > 3 and EF > 10. These thresholds correspond to considerable contamination and severe enrichment from anthropogenic sources, respectively. The maps also delineate the distribution of the Nova Lima group lithology, which is known to contribute to higher concentrations of PTEs in the basin.

Samples with EF > 10 and CF > 3 for As and Cd are concentrated in the headwater of the basin, near Ouro Preto. In this region, elevated EF values were also recorded for Cu, Zn, Pb, Cr, and Ni. However, the central portion of the basin, particularly in Rio Acima, Nova Lima, Caeté, and Sabará, presents a higher density of samples with elevated EF and CF values, primarily for As, Cd, and Cu. These areas experience considerable anthropogenic influence and are geologically dominated by the carbonate–quartz–schist of the Nova Lima group.

In Nova Lima, the highest EF and CF values for As were identified in rural communities, such as Honório Bicalho, a finding corroborated by earlier studies [22,24]. Similarly, Cd showed its peak levels (CF = 14.4 and EF = 21.9) in the Caeté region. Both elements demonstrated overlapping spatial distribution, with their highest concentrations recorded in similar areas.

The contamination by As is strongly linked to the presence of Nova Lima group rocks, rich in sulfide deposits, and historical and ongoing gold mining activities. These activities, prominent between the 17th and 19th centuries, have left a legacy of abandoned mines and tailings piles that continue to impact the environment.

Cr and Ni exhibited comparable spatial patterns, with their highest EF values concentrated in the basin's headwaters, where rocks from the Nova Lima group dominate. Cu, being a chalcophile, shares a similar spatial presence with As, reflecting its association with Nova Lima group lithology and its typical Cu-As-Ni-Cr geochemical signature.

Pb presented the highest EF levels in the southwestern part of the basin, particularly in the Mata Porcos Creek watershed. This area is heavily influenced by six active mining operations, which notably contribute to Pb release into the environment. Pb concentrations were correlated with Fe, likely due to its association with magnetite and co-precipitation processes involving Fe compounds [54,65]. Zn, while exhibiting a similar spatial distribution to Pb, has fewer points with EF > 3.

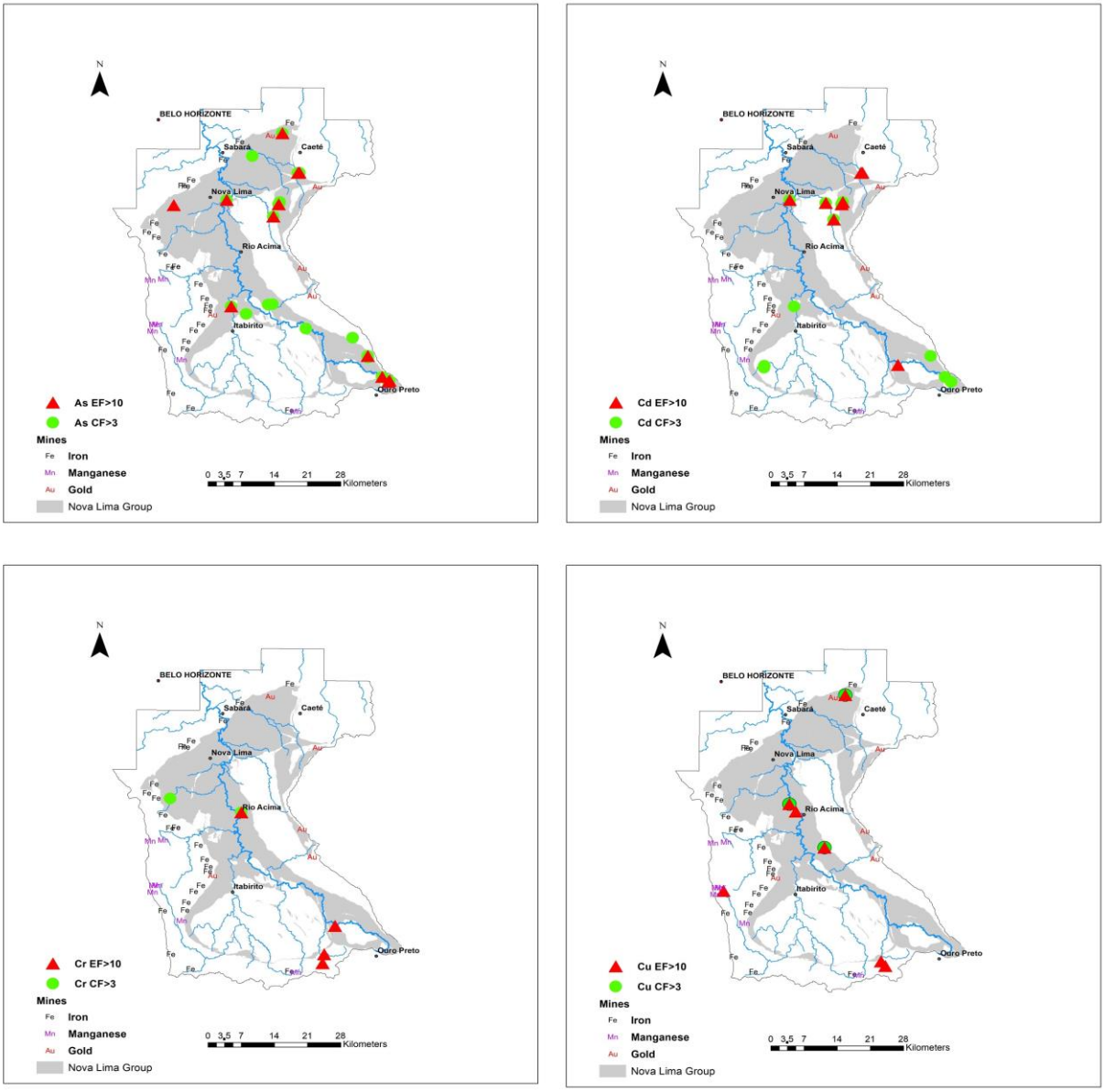

(**a**)

Figure 2. *Cont.*

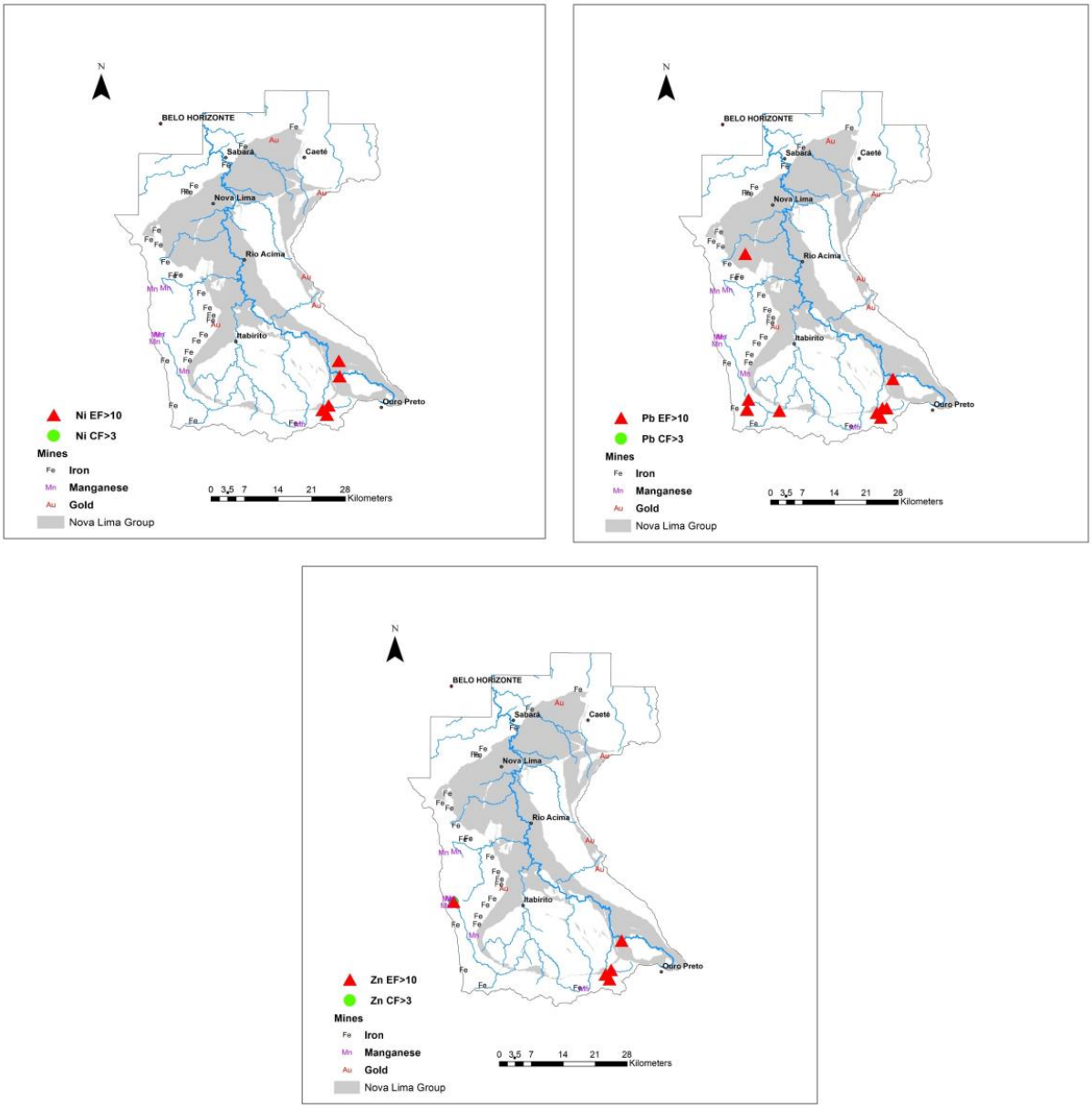

(**b**)

Figure 2. (**a**) Maps with spatial distributions of occurrences of CF > 3 and EF > 10 of single-element (As, Cd, Cr, Cu); (**b**) Maps with spatial distributions of occurrences of CF > 3 and EF > 10 of single-element (Ni, Pb, and Zn).

Although both CF and EF indicate contamination, CF tends to show higher proportions of uncontaminated samples while identifying more points with very high contamination levels for As, Cr, and Cu. This discrepancy suggests that CF may have lower sensitivity in evaluating contamination, particularly in complex geological and environmental settings. In contrast, EF provides a more detailed spatial representation due to its normalization with Al, which reduces the variability associated with natural geochemical conditions [47,53]. Previous studies [8,15] confirm that EF is better suited for identifying subtle contamination trends, underscoring the limitations of CF in such complex environments.

3.3. Sediment Quality Assessment by Multielemental Pollution Indexes

The multielement indices revealed distinct insights into sediment quality, as shown in Table 9. The modified contamination degree (mCd) ranged from 0.2 to 16.8, while the

PI and MPI demonstrated broader ranges, from 0.3 to 60.7 and 0.3 to 163.3, respectively. This disparity arises from the distinct methodology used to calculate each index, with PI and MPI incorporating maximum values in their formulas, thereby amplifying the final values. According to the mCd classification, 87% of the sediment samples were categorized as non-polluted, a proportion considerably higher than those determined by PI (18.5%) and MPI 1 (21.3%).

Table 9. Minimum and maximum mCD, PI, and MPI values for PTEs and percentage of samples in each mCD, PI, and MPI class—Velhas River basin.

Values	%mCD	%PI	%MPI
Minimum	0.2	0.3	0.3
Maximum	16.8	60.7	163.3
Percentage of Element Samples by Class			
No Pollution	86.9	18.5	21.3
Slightly Polluted	6	21.8	16.9
Moderate Pollution	4.4	41.7	14.8
Moderate to Strong Pollution	2.2	---	18.6
Severe Pollution	0.50	6.5	17.5
Strong Pollution	0	11.5	10.9
Extreme Pollution	0	---	---

In contrast, when examining polluted samples, mCd classified only 0.5% of samples as severely polluted and did not identify any sample in the strong pollution range. In comparison, PI and MPI identified 18% and 28.4% of the samples, respectively, as having severe or strong pollution. These discrepancies highlight the variability in the sensitivity and classification thresholds among the indices.

The integrated analysis of these indices reveals overlapping areas of substantial pollution. Specifically, points with PI values above five and mCd values higher than four were observed in the Ouro Preto, Itabirito, Nova Lima, and Caeté regions. These locations also correspond to areas with MPI values exceeding 12, suggesting a consistent spatial pattern of contamination.

Among the indices, mCd appears to overestimate the proportion of sediment samples classified as non-polluted. This discrepancy arises from the higher thresholds required for mCd to indicate pollution, which are comparatively lower in PI and MPI [15]. Consequently, PI and MPI identified a larger fraction of polluted samples. Notably, MPI demonstrated greater sensitivity, effectively classifying sediment samples across all pollution categories. This characteristic makes MPI particularly advantageous for evaluating complex geochemical environments, as it incorporates enrichment factors normalized by Al.

In summary, while mCd provides a conservative pollution estimate, MPI is a more robust tool for assessing sediment quality in the Velhas River basin. Its ability to normalize elemental data and classify pollution across a comprehensive range of categories makes it especially valuable for understanding contamination dynamics in complex mining-impacted environments. Table 10 summarizes the ecological risk potential (Er) for each element and the ecological risk index (RI) for all analyzed sediments in the Velhas River basin.

Approximately 96% of the analyzed trace elements (excluding As and Cd) were classified as presenting a low ecological risk at all sampled locations (Er < 40). However, As and Cd stood out for their elevated Er values, with 4.4% and 6.6% of the samples, respectively, falling into the categories of considerable to very high contamination.

The RI values varied considerably, ranging from 7.1 to 1092.2, with 3.9% of the samples exhibiting a considerable to high ecological risk. Spatial analysis of RI highlighted clusters of sampling points with high RI values (316 to 446) located in the municipalities of Ouro Preto, Caeté, and Itabirito. The highest RI value (1092.2) was recorded in Nova Lima,

near abandoned gold mining tailings, underscoring the contribution of historical mining activities to contamination in an area with gold mining tailings.

Table 10. Minimum and maximum Er and RI values for PTEs and percentage of samples in each Er and RI class—Velhas River basin.

Values	As	Cd	Cr	Cu	Pb	Zn	RI
Minimum	0.8	1.3	0.1	0.04	0.07	0.3	7.1
Maximum	820.9	433.2	2.2	30.8	12.3	2.0	1092.2
Percentage of Element Samples by Class							
Low Contamination	91.8	83.6	100	100	100	100	92.3
Moderate Contamination	3.8	9.8	0.0	0.0	0.0	0.0	3.8
Considerable Contamination	2.8	2.2	0.0	0.0	0.0	0.0	3.4
High Contamination	1.1	3.8	0.0	0.0	0.0	0.0	0.5
Very High Contamination	0.5	0.6	0.0	0.0	0.0	0.0	0.0

The high Er values for As and Cd predominantly drove the elevated RI values. These two elements showed mean Er values of 17.7 and 33, respectively, markedly higher than those of the other analyzed elements, whose average RI values ranged between 0.90 and 4.12. Cd, recognized as a highly toxic and persistent element, is often found in elevated concentrations in sediments and soils near mining regions [66,67]. Its toxicity is of particular concern due to its potential to bioaccumulate benthic organisms and propagate through the food chain, ultimately impacting aquatic ecosystems and human health [68,69].

3.4. Spatial Distribution of Multielement Quality Indexes

The spatial distribution of the multielement indices (mCd, PI, MPI, and RI) in the Velhas River basin, overlaid with the mining concession areas for Au, Fe, and Mn, reveals critical contamination hotspots (Figure 3).

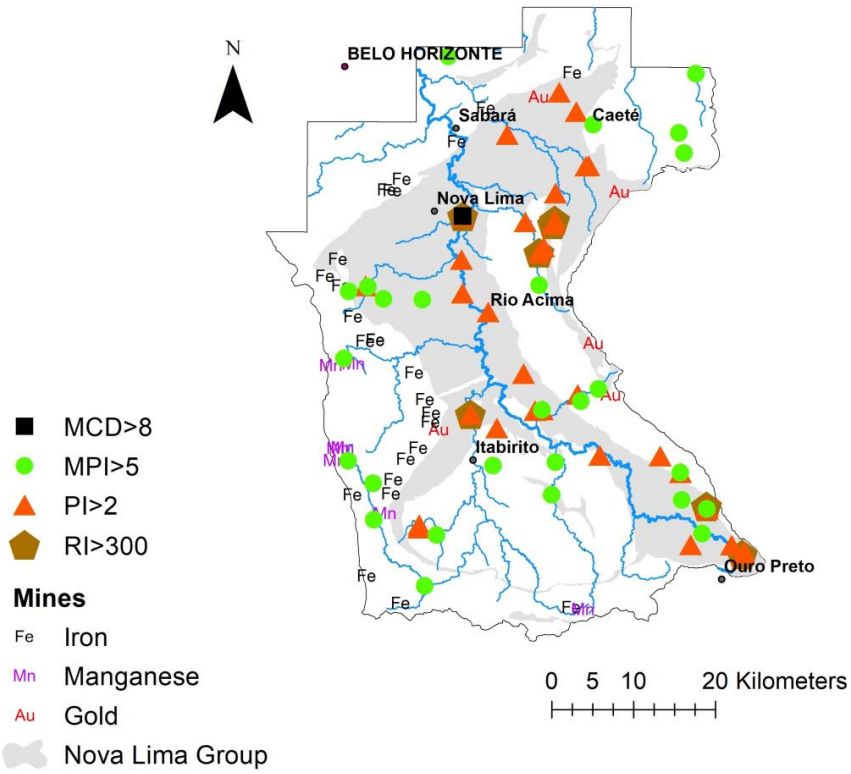

Figure 3. Map showing the distribution of mining concession areas for Fe and/or Mn and Au, suspended mining activities for Fe and Au, and occurrence of samples with mCd > 8, PI > 2, MPI > 5, and RI > 300.

The results indicate a prominent area of contamination extending from the basin's headwaters near Ouro Preto, through Itabirito, Nova Lima, and Caeté. This region has been historically impacted by mining operations, as reflected in the dense clustering of mining concession areas. The association between gold mining concessions and the Nova Lima group lithology is particularly evident, highlighting their contribution to contamination. Elevated values of mCd, PI, and MPI are concentrated in these areas, suggesting a strong relationship between mining activities and pollution levels.

The analysis focused on sites exceeding thresholds indicative of severe pollution, with mCd > 8, PI > 2, MPI > 5, and RI > 300.

4. Conclusions

The present study represents a comprehensive calculation of PTE contamination indices across the Velhas River basin, the most polluted in Minas Gerais, and located in one of the world's most important mining provinces. The high sampling density enabled a detailed evaluation of lithological controls on sediment geochemistry, revealing well-defined patterns in elemental behavior.

Intense contamination of As and Cd was identified across large portions of the basin, with two areas consistently showing high contamination across all analyzed parameters. The first is centered on the municipalities of Ouro Preto and Mariana, while the second encompasses Rio Acima, Nova Lima, Caeté, and Sabará.

The elevated concentrations of these elements in these regions are closely linked to the geology, mainly the carbonate–quartzite–schist rocks of the Nova Lima group, as well as centuries of mining activity since the 18th century and rapid urbanization over the past four decades. While many points near mining areas are monitored according to environmental legislation, this study revealed high uni- and multielement index values in areas influenced by the natural weathering of geological materials. For the first time, detailed geochemical mapping has delineated these risks, which are not currently monitored.

Previous studies in the basin highlighted high levels of As and Cd contamination, but this study advances the understanding by applying contamination indices that account for regional background values, effectively distinguishing natural from anthropogenic contributions. The geochemical maps created in this study provide a more effective environmental assessment tool, pinpointing critical contamination hotspots and identifying rural communities and urban areas exposed to severe environmental risks. These findings underscore the need for relevant authorities to intervene and take protective measures.

In conclusion, this study provides a robust foundation for targeted environmental management in the Velhas River basin, emphasizing the need for comprehensive monitoring and remediation to mitigate the risks posed by PTE contamination.

Author Contributions: Conceptualization, R.V., T.V., M.G.P.L., L.P.L. and H.A.N.J.; Methodology, R.V., M.G.P.L. and L.P.L.; Validation, R.V. and T.V.; Writing—original draft, R.V., T.V., M.G.P.L., L.P.L., H.A.N.J., P.G. and R.F.; Supervision, R.V., T.V. and M.G.P.L. All authors have read and agreed to the published version of the manuscript.

Funding: The work is funded by national funds through the FCT—Fundação para a Ciência e Tecnologia—I.P., in the framework of the UIDB/04683 and UIDP/04683—Instituto de Ciências da Terra programs. The authors highly appreciate the financial support of the institutions CNPq, FAPEMIG, and mainly CAPES for the scholarship Proc. no 10228/13-6.

Data Availability Statement: Data are contained within the article.

Acknowledgments: The authors highly appreciate the valuable comments of the anonymous reviewers.

Conflicts of Interest: The authors declare no conflicts of interest.

References

1. Liu, M.; Chen, J.; Sun, X.; Hu, Z.; Fan, D. Accumulation and transformation of heavy metals in surface sediments from the Yangtze River estuary to the East China Sea shelf. *Environ. Pollut.* **2019**, *245*, 111–121. [CrossRef] [PubMed]
2. Vicente, V.A.S.; Pinto, M.C.; Dinis, P.; Pratas, J.A.M.S. Ecological and Human Health Risk Assessment Based on Stream Sediments from Coastal Oecusse (Timor). *Water* **2024**, *16*, 3020. [CrossRef]
3. Walling, D.E. Human impact on land–ocean sediment transfer by the world's Rivers. *Geomorphology* **2006**, *79*, 192–216. [CrossRef]
4. Zhang, Z.; Lua, Y.; Li, H.; Tua, Y.; Liua, B.; Yang, Z. Assessment of heavy metal contamination, distribution and source identification in the sediments from the Zijiang River. *China Sci. Total Environ.* **2018**, *645*, 235–243. [CrossRef] [PubMed]
5. Fu, F.; Wang, Q. Removal of heavy metal ions from wastewaters: A review. *J. Environ. Manag.* **2011**, *92*, 407–418. [CrossRef]
6. Garrett, R.; Reimann, C.; Smith, D.; Xie, X. From geochemical prospecting to international geochemical mapping: A historical overview. *Geochem. Explor. Environ. Anal.* **2008**, *8*, 205–217. [CrossRef]
7. Cabral Pinto, M.M.; Ferreira da Silva, E.A. Heavy Metals of Santiago Island (Cape Verde) alluvial deposits: Baseline value maps and human health risk assessment. *Int. J. Environ. Res. Public Health* **2019**, *16*, 2. [CrossRef]
8. Çevik, F.; Göksu, M.Z.L.; Derici, O.B.; Fındık, Ö. An assessment of metal pollution in surface sediments of Seyhan dam by using enrichment factor, geoaccumulation index and statistical analyses. *Environ. Monit. Assess.* **2009**, *152*, 309–317. [CrossRef]
9. de Vicq, R.; Matschullat, J.; Leite, M.G.P.; Junior, H.A.N.; Mendonça, F.P.C. Iron Quadrangle stream sediments, Brazil: Geochemical maps and reference values. *Environ. Earth Sci.* **2015**, *74*, 4407–4417. [CrossRef]
10. Jahan, S.; Strezov, V. Comparison of pollution indices for the assessment of heavy metals in the sediments of seaports of NSW, Australia. *Mar. Pollut. Bull.* **2019**, *128*, 295–306. [CrossRef]
11. Matschullat, J.; Borba, R.P.; Deschamps, E.; Figueiredo, B.F.; Ga-Brio, T.; Schwenk, M. Human and environmental contamination in the Quadrilátero Ferrífero, Brazil. *Appl. Geochem.* **2000**, *15*, 181–190. [CrossRef]
12. Leão, L.P. Mapeamento Geoquímico de Sedimentos Fluviais: Diferentes Métodos e suas Aplicações Ambientais. Ph.D. Thesis, Programa de Pós-Graduação em Evolução Crustal e Recursos Naturais, Departamento de Geologia, Escola de Minas, Universidade Federal de Ouro Preto, Ouro Preto, Brazil, 2019.
13. MacDonald, D.D.; Ingersoll, C.G.; Berger, T.A. Development and evaluation of consensus-based sediment quality guidelines for freshwater ecosystems. *Arch. Environ. Contam. Toxicol.* **2000**, *39*, 20–31. [CrossRef] [PubMed]
14. Deckere, E.; De Cooman, W.; Leloup, V.; Meire, P.; Schmitt, C.; von der Ohe, P.C. Development of sediment quality guidelines for freshwater ecosystems. *J. Soils Sediments* **2011**, *11*, 504–517. [CrossRef]
15. Duodu, G.O.; Goonetilleke, A.; Ayoko, G.A. Comparison of pollution indices for the assessment of heavy metal in Brisbane River sediment. *Environ. Pollut.* **2016**, *219*, 1077–1091. [CrossRef]
16. Müller, G. Index of geoaccumulation in the sediments of the Rhine River. *Geojournal* **1969**, *2*, 108–118.
17. Håkanson, L. An ecological risk index for aquatic pollution control. A sedimentological approach. *Water Res.* **1980**, *14*, 975–1001. [CrossRef]
18. Ridgway, J.; Shimmield, G. Estuaries as repositories of historical contamination and their impact on shelf seas. *Estuar. Coast. Shelf Sci.* **2002**, *55*, 903–928. [CrossRef]
19. Abrahim, G.M.S.; Parker, R.J. Assessment of heavy metal enrichment factors and the degree of contamination in marine sediments from Tamaki Estuary, Auckland, New Zealand. *Environ. Monit. Assess.* **2008**, *136*, 227–238. [CrossRef]
20. Hilton, J.; Davison, W.; Ochsenbein, U. A mathematical model for analysis of sediment coke data. *Chem. Geol.* **1985**, *48*, 281–291. [CrossRef]
21. Borba, R.P.; Figueiredo, B.R.; Rawlins, B.; Matschullat, J. Arsenic in Water and Sediment in the Iron Quadrangle, State of Minas Gerais, Brazil. *Appl. Geochem.* **2000**, *15*, 181–190. [CrossRef]
22. Deschamps, E.; Matschullat, J. *Arsênio Antropogênico e Natural: Um Estudo em Regiões do Quadrilátero Ferrífero*; Fundação Estadual do Meio Ambiente—FEAM, Belo Horizonte: Minas Gerais, Brazil, 2007; p. 330.
23. Pereira, J.C.; Guimarães Silva, A.K.; Nalini, H.A., Jr.; Pacheco Silva, E.; De Lena, J.C. Distribuição, fracionamento e mobilidade de elementos traço em sedimentos superficiais. *Quim. Nova* **2007**, *30*, 1249–1255. [CrossRef]
24. APA Sul RMBH. 2005. Projeto de Geoquímica Ambiental, Mapas Geoquímicos Escala 1:225.000. Fernanda G. da Cunha, Gilberto J. Machado—Belo Horizonte: Secretaria Estadual Meio Ambiente e Companhia de Pesquisa de Recursos Minerais. 80p., v. 7: 17 Mapas (Série Programa Informações Básicas para a Gestão Territorial—GATE). Available online: https://rigeo.sgb.gov.br/bitstream/doc/10218/16/rel_apa_sulrmbhv1.pdf (accessed on 10 February 2025).
25. Gonçalves, G.H.T. Avaliação Geoambiental de Bacias Contíguas Situadas na Área de Proteção Ambiental Cachoeira das Andorinhas e Floresta Estadual do Uaimii, Ouro Preto-MG: Diagnóstico e Percepção Ambiental. Master's Thesis, Escola de Minas, Departamento de Geologia, Programa de Pós-graduação em Evolução Crustal e Recursos Naturais, Universidade Federal de Ouro Preto, Preto, Brazil, 2010.

26. Mendonça, F.P.C. Influência da Mineração na Geoquímica das Águas Superficiais e nos Sedimentos no Alto Curso da Bacia do Ribeirão Mata Porcos, Quadrilátero Ferrífero—Minas Gerais. Master's Thesis, Escola de Minas, Departamento de Geologia, Programa de Pós-Graduação em Evolução Crustal e Recursos Naturais, Universidade Federal de Ouro Preto, Preto, Brazil, 2012.
27. Instituto Brasileiro de Geografia e Estatística (IBGE) Censo Demográfico do Brasil. 2021. Available online: https://censo2022.ibge.gov.br/ (accessed on 15 December 2024).
28. Ladeira, E.A.; Roeser HM, P.; Tobschall, H.J. Evolução Petrogenética do Cinturão de Rochas Verdes, Rio das Velhas, Quadrilátero Ferrífero, Minas Gerais. In Proceedings of the Simpósio Geológico, Belo Horizonte, Brazil, 10–14 August 1983; pp. 149–165.
29. Teixeira, W.; Sabaté, P.; Barbosa, J.; Noce, C.M.; Carneiro, M.A. Archean and paleoproterozoic tectonic evolution of the São Francisco Craton. In *Proceedings of International Geological Congress, Rio de Janeiro, 2000. Tectonic Evolution of South America*; Cordani, U.G., Milani, E.J., Thomaz Filho, A., Campos, D.A., Eds.; 31st International Geological Congress, Rio de Janeiro; 2000; Volume 31, pp. 101–137. Available online: https://rigeo.sgb.gov.br/handle/doc/19419 (accessed on 10 February 2025).
30. Dorr, J.N. Physiographic, Stratigraphic, and Structural Development of the Quadrilátero Ferrífero, Minas Gerais. U.S. Geological Survey. 1969. Professional. Paper. Available online: https://pubs.usgs.gov/pp/0641a/report.pdf (accessed on 12 December 2024).
31. Alkmim, F.F.; Marshak, S. Transamazonian Orogeny in the Southern São Francisco Craton Region, Minas Gerais, Brazil: Evidence for Paleoproterozoic collision and collapse in the Quadrilátero Ferrífero. *Precambrian Res.* **1998**, *90*, 29–58. [CrossRef]
32. Nalini, H.A., Jr. *Estudosgeoambientais no Quadrilátero Ferrífero: Mineração e Sustentabilidade*; School of Mines, Department of Geology, Escola de Minas, Universidade Federal de Ouro Preto: Minas Gerais, Brazil, 2009; p. 52.
33. Zucchetti, M.; Baltazar, O.F. Projeto Rio das Velhas: Texto Explicativo do Mapa Geológico Integrado—Escala 1:100.000/Organizado por DNPM/CPRM—Belo Horizonte, 2a Reimpressão. 2000. Available online: https://rigeo.sgb.gov.br/bitstream/doc/22798/1/rio%20da%20velhas_2000.pdf (accessed on 7 February 2025).
34. Vieira, F.W.R.; Oliveira, G.A.I. Geologia do Distrito Aurífero de Nova Lima, Minas Gerais. In *Principais Depósitos Minerais do Brasil*; Schobbenhaus, C., Coelho, C.E.S., Eds.; DNPM/CVRD: Brasília, Brazil, 1988; Volume 3, pp. 377–391.
35. Roeser, H.M.P.; Roeser, P.A. O Quadrilátero Ferrífero-MG, Brasil: Aspectos Sobre sua História, Seus Recursos Minerais e Problemas Ambientais Relacionados. Geonomos. 2010. Available online: https://periodicos.ufmg.br/index.php/revistageonomos/article/view/11598 (accessed on 25 January 2025).
36. Anuário Mineral Brasileiro: Principais Substâncias Metálicas/Agência Nacional de Mineração; Coordenação Técnica de Marina Dalla Costa—Brasília: ANM. 2022; 30p. Available online: https://www.gov.br/anm/pt-br/assuntos/economia-mineral/publicacoes/anuario-mineral/anuario-mineral-brasileiro/PreviaAMB2022.pdf (accessed on 26 January 2025).
37. Bølviken, B.; Bogen, J.; Jartun, M.; Langedal, M.; Ottesen, R.; Volden, T. Overbank sediments: A natural bed blending sampling medium for large-scale geochemical mapping. *Chemom. Intell. Lab. Syst.* **2004**, *74*, 183–199. [CrossRef]
38. Salminen, R.; Tarvainen, T.; Demetriades, A.; Duris, M.; Fordyce, F.M.; Gregorauskiene, V.; Kahelin, H.; Kivisilla, J.; Klaver, G.; Klein, H.; et al. *FOREGS Geochemical Mapping Field Manual. Guide 47*; Geological Survey of Finland: Espoo, Finland, 1998; p. 36.
39. United States Environmental Protection Agency (USEPA) Method 3005A—Acid Digestion of Waters for Total Recoverable or Dissolved Metals for Analysis by FLAA or ICP Spectroscopy. 2001; p. 5. Available online: https://www.epa.gov/sites/default/files/2015-12/documents/3005a.pdf (accessed on 16 December 2024).
40. Calmano, W.; Förstner, U. *Sediments and Toxic Substances: Environmental Effects and Ecotoxicity, 1st ed*; Springer: Berlin/Heidelberg, Germany, 1996; p. 332.
41. Ferreira, A.; Inácio, M.; Morgado, P.; Batista, M.; Ferreira, L.; Pereira, V.; Pinto, M. Low-density geochemical mapping in Portugal. *Appl. Geochem.* **2001**, *16*, 1323–1331. [CrossRef]
42. Albanese, S.S.; De Vivo, B.; Lima, A.; Cicchella, D. Geochemical background and baseline values of toxic elements in stream sediments of Campania region (Italy). *J. Geochem. Explor.* **2006**, *93*, 21–34. [CrossRef]
43. Vicq, R.; Leite, M.G.P.; Leão, L.P.; Júnior, H.A.N.; Valente, T. Geochemical Mapping and Reference Values of Potentially Toxic Elements in a Contaminated Mining Region: Upper Velhas River Basin Stream Sediments, Iron Quadrangle, Brazil. *Minerals* **2023**, *13*, 1545. [CrossRef]
44. Reimann, C.; de Caritat, P. Distinguishing between natural and anthropogenic sources for elements in the environment: Regional geochemical surveys versus enrichment factors. *Sci. Total. Environ.* **2005**, *337*, 91–107. [CrossRef]
45. Wedepohl, K.H. The composition of the continental crust. *Geochim. Cosmochim. Acta* **1995**, *59*, 1217–1232. [CrossRef]
46. Birch, G. An assessment of aluminum and iron in normalisation and enrichment procedures for environmental assessment of marine sediment. *Sci. Total. Environ.* **2020**, *727*, 138123. [CrossRef]
47. Birch, G. A review and critical assessment of sedimentary metal indices used in determining the magnitude of anthropogenic change in coastal environments. *Sci. Total. Environ.* **2023**, *854*, 158129. [CrossRef]
48. Balls, P.; Hull, S.; Miller, B.; Pirie, J.; Proctor, W. Trace metal in Scottish estuarine and coastal sediments. *Mar. Pollut. Bull.* **1997**, *34*, 42–50. [CrossRef]

49. Muñoz-Barbosa, A.; Huerta-Diaz, M.A. Trace metal enrichments in nearshore sediments and accumulation in mussels (Modiolus capax) along the eastern coast of Baja California, Mexico: Environmental status in 1995. *Mar. Pollut. Bull.* **2013**, *77*, 71–81. [CrossRef] [PubMed]
50. Rubio, B.; Nombella, M.A.; Vilas, F. Geochemistry of major and trace elements in sediments of the Ria de Vigo (NWSpain): An assessment of metal pollution. *Mar. Pollut. Bull.* **2000**, *40*, 968–980. [CrossRef]
51. Nolting, R.F.; Ramkema, A.; Everaarts, J.M. The geochemistry of Cu, Cd, Zn, Ni and Pb in sediment cores from the continental slope of the Banc d'Arguin (Mauritania). *Cont. Shelf Res.* **1999**, *19*, 665–691. [CrossRef]
52. Nemerow, N.L. *Stream, Lake, Estuary, and Ocean Pollution*; Van Nostrand Reinhold: New York, NY, USA, 1991.
53. Brady, J.P.; Ayoko, G.A.; Martens, W.N.; Goonetilleke, A. Development of a hybrid pollution index for heavy metals in marine and estuarine sediments. *Environ. Monit. Assess.* **2015**, *187*, 306. [CrossRef]
54. Reimann, C.; Caritat, P. *Chemical Elements in the Environment: Factsheets for the Geochemist and Environmental Scientist*; Springer: Berlin/Heidelberg, Germany, 1998; p. 398.
55. Ke, X.; Gui, S.; Huang, H.; Zhan, H.; Wang, C.; Guo, W. Ecological risk assessment and source identification for heavy metals in surface sediment from the Liaohe River protected area, China. *Chemosphere* **2017**, *175*, 473–481. [CrossRef]
56. Wang, L.; Liang, T. Geochemical fractions of rare earth elements in soil around a mine tailing in Baotou, China. *Sci. Rep.* **2015**, *5*, 12483. [CrossRef]
57. Varol, M. Assessment of heavy metal contamination in sediments of the Tigris River (Turkey) using pollution índices and multivariate statistical techniques. *J. Hazard. Mater.* **2011**, *195*, 355–364. [CrossRef]
58. Woitke, P.; Wellmitz, J.; Helm, D.; Kube, P.; Lepom, P.; Litheraty, P. Analysis and assessment of heavy metal pollution in suspended solids and sediments of the river Danube. *Chemosphere* **2003**, *51*, 633–642. [CrossRef]
59. Karageorgis, A.; Nikolaidis, N.; Karamanos, H.; Skoulikidis, N. Water and sediment quality assessment of the Axios River and its coastal environment. *Cont. Shelf Res.* **2003**, *23*, 1929–1944. [CrossRef]
60. Heiny, J.S.; Tate, C.M. Concentration, distribution, and comparison of selected trace elements in bed sediment and fish tissue in the South Platte River Basin, USA, 1992–1993. *Arch. Environ. Contam. Toxicol.* **1997**, *32*, 246–259. [CrossRef] [PubMed]
61. Mendez, W. *Contamination of Rimac River Basin, Peru, due to Mining Tailings, TRITALWR, MS Dissertation, Environmental Engineering and Sustainable Infrastructure*; The Royal Institute of Technology (KTH): Stockholm, Sweden, 2005.
62. Liu, X.; Jiang, J.; Yan, Y.; Dai, Y.Y.; Deng, B.; Ding, S.; Su, S.; Sun, W.; Li, Z.; Gan, Z. Distribution and risk assessment of metals in water, sediments, and wild fish from Luan River, China. *Chemosphere* **2018**, *196*, 45–52. [CrossRef] [PubMed]
63. Gomes, P.; Valente, T. (In Press). Potential Accumulation of Strategic Elements in Mining Dams—From Remining to Rehabilitation. Special Issue "Congresso Nacional de Geologia". Comunicações Geológicas. Available online: https://portaberta.uminho.pt/display/cv-t-c5f77356040f5772681a5b4b1097ad98 (accessed on 10 February 2025).
64. Environment Canada, Guidelines Division Technical Secretariat of the CCME Task Group on Water Quality Guidelines, Ottawa. 2003. EPC-98E. CCME (Canadian Council of Ministers of the Environment) Protocol for the Derivation of Canadian Sediment Quality Guidelines for the Protection of Aquatic Life. 2003. Available online: https://ccme.ca/en/resources/sediment (accessed on 10 February 2025).
65. Merian, E.; Anke, M.; Ihnat, M.; Stoeppler, M. *Elements and Their Compounds in the Environment: Occurrence, Analysis and Biological Relevance*; WILEY-VCH: Weinheim, Germany, 2004; p. 1773.
66. Zheng-Qi, X.; Shi-Jun, N.; Xian-Guo, T.; Cheng-Jiang, Z. Calculation of heavy metals' toxicity coefficient in the evaluation of potential ecological risk index. *Environ. Sci. Technol.* **2008**, *31*, 112–115.
67. Pan, Y.; Li, H. Investigating heavy metal pollution in mining brownfield and its policy implications: A case study of the Bayan Obo rare Earth mine, Inner Mongolia. *China. Environ. Manag.* **2016**, *57*, 879–893. [CrossRef]
68. Olayinka-Olagunju, J.O.; Dosumu, A.A.; Olatunji-Ojo, A.M. Bioaccumulation of heavy metals in pelagic and benthic fishes of Ogbese River, Ondo State, South-Western Nigeria. *Water Air Soil Pollut.* **2021**, *232*, 44. [CrossRef]
69. Muhammad, S.; Ali, W.; Rehman, I.U. Potentially harmful elements accumulation and health risk assessment of edible fish tissues caught from the Phander Valley, Northern Pakistan. *Biol. Trace Elem. Res.* **2021**, *200*, 4837–4845. [CrossRef]

Disclaimer/Publisher's Note: The statements, opinions and data contained in all publications are solely those of the individual author(s) and contributor(s) and not of MDPI and/or the editor(s). MDPI and/or the editor(s) disclaim responsibility for any injury to people or property resulting from any ideas, methods, instructions or products referred to in the content.